INDENTATION CREEP AS A THERMALLY ACTIVATED PROCESS

By
KOASHAL KISHOR MANI PANDEY

MATERIALS SCIENCE PROGRAMME
INDIAN INSTITUTE OF TECHNOLOGY, KANPUR
June, 2000

INDENTATION CREEP AS A THERMALLY ACTIVATED PROCESS

A Thesis Submitted
in Partial Fulfillment of the Requirements
for the Degree of

MASTER OF TECHNOLOGY

By

KOASHAL KISHOR MANI PANDEY

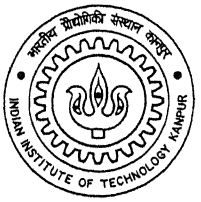

to the

MATERIAL SCIENCE PROGRAMME

INDIAN INSTITUTE OF TECHNOLOGY KANPUR

JUNE, 2000


DEDICATED
TO
MOTHER

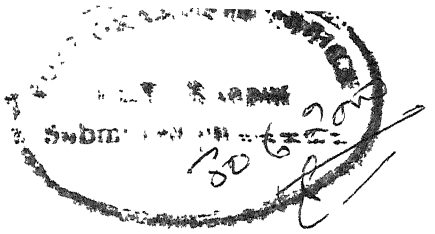

Certificate

It is to certify that the work contained in the thesis entitled ***"Indentation Creep as a Thermally Activated Process"*** by Koashal Kishor Mani Pandey has been carried out under my supervision and that this work has not been submitted elsewhere for a degree.

Om Prakash
30/6/00

(June, 2000)

(Dr. Om Prakash)

Astt. Professor
Department of Mechanical Engineering
Indian Institute of Technology
Kanpur – 208016
India.

Acknowledgement

At the very outset I wish to express my deep sense of gratitude to Dr. Om Prakash for his invaluable guidance and encouragement throughout the thesis work.

I am highly obliged to Prof. Jitendra Kumar, Prof. D.C. Agrawal, Prof. K Shahi, Prof. K.N. Rai and all non-teaching staff of the department for their outstanding contribution.

I thank my colleagues Amit, Ramanujam, S.Baba, Srikanth, S.D.Dube and Priyanka, who played an active role in the completion of my M.Tech. dissertation.

I also thank to Anupam Chandra, Akash, Manish, Sunit, Shobhit, J. Choudhary, and SP. with whom I spent the best days of my life at IITK.

The acknowledgement remains incomplete without the mention of my family members, especially my uncle Mr. Narendra Pandey for their moral support and inspiration.

Last but not the least, I would like to express my thanks to CSIR for financial assistantship during M.Tech. programme.

Koashal Kishor Mani Pandey

INDENTATION CREEP AS A THERMALLY ACTIVATED PROCESS

Name of the student: K. K. M. Pandey
Program: M. Tech., Materials Science Program
Indian Institute of Technology, Kanpur
Date: June 2000

ABSTRACT

This work deals with modeling of indentation creep as a thermally activated process. A procedure, which takes into account the thermally activated nature of creep deformation, has been developed to analyse indentation creep. The procedure allows determination of activation volume from time and temperature dependent hardness data.

The model has been applied to various materials for which experimental (indentation creep) data is available in literature. The materials considered in this study are AgCl, LiF, UO_2, Si, Ge, and Fe. The results have been compared with activation volume data based on uniaxial creep studies. Good agreement is obtained between our results and earlier data supporting the validity of the proposed approach.

Contents

Page No.

List of Figures — Page No.

List of Table Page No.

List of Symbols

D_B	grain boundary diffusion coefficient
D_v	bulk diffusion coefficient
H	hardness
H	strain hardening rate
Q	activation energy
R	recovery rate
T	temperature in absolute scale
T_m	absolute melting point
V_a	activation volume
b	Burger vector
d	grain size
k_B	Boltzman constant
n	stress exponent
v	dislocation velocity
Ω	atomic volume
δ	effective cross-section for grain boundary
ε	strain at time t
$\dot{\varepsilon}$	strain rate
ε_0	strain at time t=0
ε_s	steady state strain rate
ρ_m	dislocation density
μ	shear modulous
ν^+	frequency for forward jump
ν^-	frequency for backward jump

ν net forward frequency

ν_0 attempt frequency

σ applied stress

σ_b internal stress

Chapter 1

INTRODUCTION

The physics of high temperature plastic deformation of solids has long been an object of interest for mechanical engineer, physicists and material scientists. The motivation for such studies is to develop an understanding of the underlying mechanisms so as to develop new materials with greater high temperature strength properties. A related issue is the development of experimental techniques and analytical models to characterize the mechanical response of such materials. For example, development of new materials in the form of thin films, microelectronic and MEMS (micro electro mechanical systems) devices, nanocrystalline materials etc. require testing procedure different from the conventional tests which are performed on bulk solids. The work described in this thesis deals with one such technique, indentation creep, which has been developed to understand creep behavior of materials in terms of time and temperature dependent hardness data.

Creep is permanent time dependent deformation of material under load. It is usually associated with high temperature (above 0.3 T_m, where T_m is absolute melting temperature of material). An understanding of creep is important for design of engineering components for high temperature applications such as power-plant, air craft engine, nuclear

reactor, oil refineries, boiler, steam turbine etc., which operate at temperature up to 800-1000^{0}C. Increasing demand of modern technology require materials with even better high temperature strength and oxidation resistance. The strength of material can be improved only when the underlying deformation mechanism are understood. Accordingly, a brief overview of the various creep processes and mechanisms has been summarized in chapter two.

The creep properties of a material is generally determined using uniaxial creep test where the elongation of a tensile specimen is measured with time at constant stress or load. The response is obtained at various load and temperatures. The strain rate sensitivity of temperature and stress is thus determined. Other creep techniques include test on uniaxial specimen under condition of constant strain rate and relaxation tests.

However these methods are time consuming. and are not suitable for quick evaluation of creep properties of a material. To get the information of any material, a lot of effort has to be put in. To overcome these problems indentation creep method has been developed over the years. This is discussed in detail in chapter two.

Indentation creep is the time dependent motion of hard indenter into solid under constant load. When an indenter is pressed into a hot solid, it penetrates the material, first by yielding, then by creep. The creep properties of a solid are difficult to measure particularly for materials having high melting point or those only available as small test pieces. A difficulty with indentation creep is that there is no standard creep indentation test and no fully accepted validated method of analyzing creep indentation data. The various approaches to analyzing indentation creep have been discussed in chapter two where it is pointed out that these method generally adopt power law. Since creep is a thermally activated process, it would be more appropriate to model the process in

terms of the role of thermal activation. A model has been developed in this work , and is presented in chapter three.

The validity of the proposed model has been verified in chapter four, where previously published indentation creep data of silver chloride, lithium fluoride, iron, silicon, germanium and uranium dioxide has been considered. The variations of Vickers microhardness of these materials with indentation time and test temperature are utilized to find out the activation volume.

The major findings of this work and suggestions for future work are summarized in chapter five.

CHAPTER 2

REVIEW

2.1 Brief Overview of Creep Processes

Progressive deformation of material under constant load is called creep. It is appreciable at higher temperature. When a constant uniaxial load is applied to a specimen at temperature greater than 0.3 T_m (T_m = absolute melting temperature) extensive deformation can occur with time. The repetition of the same experiment at different load leads to a quite different response as shown in Fig. 2.1.

2.1.1 Stages of Creep Deformation

Following the instantaneous strain, which occurs when the load is first applied, the creep curve normally starts with a primary creep, transient region during which the strain rate decreases with time. In compression creep test, the primary stage is usually followed by a quasi-steady state regime (secondary creep) during which creep curve can be approximated to a straight line. Eventually as the strain increases and the constraints at the platens become important, the strain rate decreases significantly (Fig. 2.2).

In tension, on other hand, the quasi-steady state regime is followed by an unstable regime, called tertiary creep during which the strain rate

increases. The specimen is associated with necking or internal void formation and finally fails (Fig. 2.3). This is because during the engineering creep test, the stress should maintain to a constant value throughout the test. But as the test specimen elongates, a decrease in cross-sectional area takes place. As a result the axial stress increases (since, stress σ = P/A where P is constant load applied and A is instantaneous cross-sectional area).

The method for compensating the change in dimension of specimen, so as to carry out the creep test under constant stress condition has been developed by Andrade et al [1] and Fullman et al [2]. When the arrangement developed in these references are employed, curve B in Fig. 2.3 is obtained, which also give constant strain rate in region III. In Fig. 2.3 solid line represent the constant load curve, instead of constant stress curve represented by dotted line.

[A] Primary Creep

Primary creep of metallic materials was first described by Andrade [3], he found that it could be fitted by equation of the form

$$\varepsilon = \varepsilon_0 + \beta\, t^{1/3} + k\, t \qquad (2.1)$$

where ε is strain at time t, ε_0 is the instantaneous strain arising due to application of stress at t = 0 and β and k are constants.

The total strain is seen as superposition of primary transient creep in $t^{1/3}$ on viscous steady state creep with creep rate k as shown in Fig. 2.4.

Later on another equation was proposed by Garofalo [4] which gives better fit than Andrade creep equation and is given by

$$\varepsilon = \varepsilon_0 + \varepsilon_t \left(1 - e^{rt}\right) + \dot{\varepsilon}_s\, t \qquad (2.2)$$

where, ε_0 is instantaneous creep strain on loading at t = 0, ε_t being limit for transient creep, r is ratio of transient creep rate and transient creep strain and $\dot{\varepsilon}_s$ is the steady state strain rate.

It was observed that creep rate in primary creep region decreases with time because the effect of work hardening is more than that of recovery and recovery does not compensate exactly for strain hardening.

[B] Steady State Creep

In steady state creep region, the creep rate is minimum and is constant with time. In this region work hardening and recovery process are exactly balanced. The steady state creep rate is usually described by power law equation given by Nortons law as given below.

$$\dot{\varepsilon}_s = A\sigma^n \exp\left(-\frac{Q}{k_B T}\right) \tag{2.3}$$

where ,$\dot{\varepsilon}_s$ is the steady state strain rate, A is a constant, σ is the applied stress, n is a constant called stress exponent, Q is the activation energy for creep, k_B is Boltzman constant and T is temperature in absolute scale.

The quantities n and Q are material characteristics and can be obtained over specific stress and temperature ranges by conducting test for many combinations of stress and temperature. The variation of stress exponent and activation energy with stress and temperature suggests that different mechanism control creep deformation in different ranges of stress and temperature.

2.2 Creep Mechanisms

The various mechanism of creep deformation are broadly divided into two categories namely dislocation creep and diffusion creep.

2.2.1 Dislocation Creep

Dislocation creep is the name given to the creep deformation that occurs by the movement of dislocations. The strain rate, $\dot{\varepsilon}$, resulting from motion of dislocations is given by Orowan [5] equation,

$$\dot{\varepsilon} = \rho_m b v \tag{2.4}$$

where, ρ_m is the density of mobile dislocation with Burger vector vector b and mean dislocation velocity v

Suitable descriptions of ρ_m and v under creep conditions can be shown to lead to creep equation such as eq. 2.3. In eq. 2.3, the stress exponent results from the stress dependence of ρ_m and v, and the temperature dependence of steady-state strain rate results from the temperature dependence of v. Because of power relationship between the steady-state strain-rate and the applied stress, dislocation creep is also called power law creep. Various models of dislocation creep differ in the way they describe the stress and temperature dependence.

Dislocation creep is usually associated with diffusion controlled recovery mechanism and is described by dynamic interaction between dislocation glide (which leads to strain hardening) and recovery. When a material is stressed, the distribution of dislocations present in the material evolves from a homogeneous low density to higher density structure of small cells separated by dislocation walls. The generation and interaction

of dislocations has been described in detail in Ref. [6-8]. The increase in dislocation density gives rise to internal back stress which resists further glide of dislocation. Recovery processes oppose this hardening of the material and there is competition between the two. This competition can be expressed by the Bailey-Orowan equation which describes the evolution of internal stress, σ_b as

$$\left(\frac{d\sigma_b}{dt}\right)_{\sigma,t} = H\dot{\varepsilon} - R \tag{2.5}$$

where H is strain hardening rate given by

$$H = \left(\frac{\partial\sigma_b}{\partial\varepsilon}\right)_{\sigma,t,T} \tag{2.6}$$

and R is recovery rate given by

$$R = -\left(\frac{\partial\sigma_b}{\partial t}\right)_{\sigma,T} \tag{2.7}$$

During primary creep, the evolution of the dislocation substructure results in a change in the strain rate. However, once a balance between the hardening and recovery rates is reached, $\left(\frac{\partial\sigma_b}{\partial t}\right)_{\sigma,T} = 0$ and the steady state is achieved. The steady-state strain rate is then given by

$$\dot{\varepsilon}_S = \frac{R}{H} \tag{2.8}$$

The recovery process is usually considered to consist of diffusion controlled dislocation climb. The activation energy for creep is then that of vacancy diffusion (Sherby and Weertman [9]). Robinson and Sherby [10] have suggested that diffusion through the dislocation core becomes important at high stresses and low temperatures. Other models consider that the cross-slip of screw dislocation [11-12] or the climb of dislocation at grain boundaries [13] could be controlling.

Recent models of dislocation creep [14-18] consider the details of dislocation substructure, which develops during deformation. The basis of these models is the generation and immobilization of dislocation at subgrain boundaries, the recovery of static dislocation at the boundaries, the dynamics of nucleation and growth of subgrain and evolution of the dislocation density in the boundaries. Since these models consider the evolution of dislocation substructure, they can describe both primary and secondary stage of dislocation creep.

2.2.2 Diffusion Creep

Diffusion creep becomes the rate controlling mechanism at high temperature and relatively low stresses. In this case polycrystalline materials deform due to vacancy diffusion. Vacancy can diffuse either through the crystal lattice or along grain boundaries. Accordingly, a distinction is made between Nabarro-Herring creep associated with lattice diffusion and Coble creep associated with diffusion through the grain boundaries. The steady state strain rate in both these processes is linearly proportional to applied stress. The equation for combined effect of Nabarro-Hearing and Coble creep for steady-state strain rate is

$$\dot{\varepsilon}_s = \frac{14\,\sigma\Omega}{k_B T}\frac{1}{d^2} D_v \left[1 + \frac{\pi\delta\, D_B}{dD_v}\right] \qquad (2.9)$$

where, Ω is the atomic volume, d the grain size, D_v the bulk diffusion coefficient, D_B the grain boundary diffusion coefficient and δ the effective cross section of grain boundary for diffusion transport.

The grain size has important effect in diffusion creep. The grain size dependence of the steady-state strain-rate is often used to distinguish between Nabarro-Herring and Coble creep behaviour. An inverse

dependence of square of grain size indicates lattice diffusion (Nabarro-Herring Creep) whereas the inverse dependence of cube of grain size indicates grain boundary diffusion (Coble Creep). The activation energy for lattice diffusion along the two paths is also different. The activation energy for lattice diffusion is the self diffusion activation energy, whereas the activation energy for grain boundary diffusion is about two third of self diffusion activation energy. The illustration and utilization of constituting equations for various creep deformation mechanisms is displayed clearly in term of deformation mechanism map as given in Fig. 2.5.

2.3 Creep as thermally activated processes

The deformation of crystalline materials at elevated temperature is thermally activated process. A crystal contains distribution of dislocations and some obstacles to their motion. Each obstacle may be characterized by critical stress σ_0, which means that at 0K this obstacle is overcome by the dislocation under an applied stress $\sigma = \sigma_0$ (an energy barrier $Q(\sigma, \sigma_0)$ can therefore be attributed to every obstacle which reduces to zero for $\sigma = \sigma_0$). If constant stress σ is applied to the crystal, obstacles with $\sigma_0 < \sigma$ will be overcome at once by the dislocation, giving rise to instantaneous strain. When temperature is different from 0K, obstacles with $\sigma_0 > \sigma$ have a chance equal to $\exp\left(-\frac{Q}{k_B T}(\sigma, \sigma_0)\right)$ per unit time and movement of dislocations is considered as thermally activated process. As soon as dislocation arrested at obstacle with σ_0 slightly higher than σ, a small value of $Q(\sigma, \sigma_0)$ will quickly enable the dislocation to overcome this

obstacle and rapid strain results. For the flow to proceeds further, stronger obstacle with large σ_0 and $Q(\sigma, \sigma_0)$ need to be overcome giving rise to slower strain rate. Under the thermally activated process the dislocation can jump over barrier with frequency ν^+, which is given by Eyring equation

$$\nu^+ = \nu_0 \exp\left(\frac{-Q + V_a\sigma}{k_B T}\right) \tag{2.10}$$

Where Q is height of energy barrier and $V_a\sigma$ is the work done by the applied stress, which help in overcoming the barrier height, ν_0 is attempt frequency and V_a is activation volume.

Once the barrier has been overcome and dislocation segments have fallen into the next trough, after that it acquires new energy to overcome the following barrier in purely random process. Thus there will be a chance to jump back with frequency

$$\nu^- = \nu_0 \exp\left(\frac{-Q + V_a\sigma}{k_B T}\right) \tag{2.11}$$

Thus the net forward reaction rate is

$$\nu = \nu^+ - \nu^-$$

$$\nu = \nu_0 \exp\left(\frac{Q}{k_B T}\right) \sinh\left(\frac{V_a\sigma}{k_B T}\right) \tag{2.12}$$

The net forward reaction rate determines the macroscopically observed creep strain rate of a specimen subjected to external loading at a specified temperature.

2.4 Indentation Creep

Indentation creep is the creep response of material when a localized load in the form of hardness indenter is applied to its surface. These tests

are of great engineering significance, since they enable the creep characterization of material much more easily and cheaply compared to conventional uniaxial creep test. A better understanding of indentation creep is important in its own right as well since macro-creep does not represent every possible situation where creep resistance is important consideration.

A question in the study of indentation creep is about the link between uniaxial and indentation creep. The steady-state creep of crystalline material under uniaxial loading is described in terms of power law given by eq. 2.3. The material characteristics n and Q are obtained over specific range of stress and temperature range by conducting tests for many combination of stress and temperature. Indentation creep in contrast, requires much less time and volume of material. A single test at given temperature provides information at various stress levels. However the details of the deformation mechanisms in the material below the indenter are not well understood. The difficulties in understanding indentation creep can be linked to the following considerations.

First of all, there is no clear definition of strain and strain rate resulting from the indentation geometry of loading. Secondly, the stress field below the indenter is very complex, and there is no unique well-defined stress, which could be used for the purpose of stress analysis. The presence of non-uniform stress field means that material at different distance from the indenter tip creeps at different rates and may creep though different mechanisms. Different creep rates at different points may lead to strain incompatibilities unless there is stress redistribution. With different mechanisms operating in different regions of material below the indenter, the problem of analyzing creep indentation data becomes even more intractable. Thirdly, it is not clear whether the creeping material is undergoing primary or steady-state creep. Finally the

effect of microstructural inhomogeneities which exist in all real material, and which may be accentuated by the highly constrained nature of deformation by indentation creep, cannot be ignored.

2.4.1 Review of indentation creep models

Initially it was assumed that the hardness number is independent of indentation time (i.e., the indenter comes to equilibrium with solid being tested within the time required to apply the full indentation load. But later on, various workers experimentally observed that the hardness of material is dependent on indentation time and temperature. The hardness of material decreases with increasing indentation time and temperature. Hargreaves [19] and Ito [20] gave a typical relation by establishing the dependence of hardness on indentation time and temperature

$$\log(H) = a - bt - cT\log(t) \qquad (2.13)$$

where, H is the time varying hardness with indentation (dwell) time t at absolute temperature T and a, b, c are constants. This equation is essentially an empirical fit to experimental data.

A number of attempts were made to link the hardness behavior of metals and non-metals with their known characteristics. After the early work which identified empirical time laws, later studies have tried to describe the indentation creep process based on various theoretical approaches. The model proposed by Mulhearn and Tabor [21] for indentation creep is based on the concept of representative strain beneath the indenter. They assumed that secondary creep controls the deformation rate, and used Norton type creep equation with stress exponent n and activation energy Q. This leads to the following equation

$$H^{n+0.5}t = A_1 \exp\left(\frac{Q}{k_B T}\right) \qquad (2.14)$$

where, A_1 is constant. However experimental evidence, Atkins [22], shows that during the indentation process, there is an increase in size of plastically deformed region, and therefore suggested a transient creep analysis. They used a primary creep law in conjunction with the expanding cavity model. The mechanism of indentation process is considered similar to the expansion of hemispherical cavity into a semi-infinite space. The essential elements of deformation and stresses around and indentation have been discussed by Tabor [23]. The basic model [24-27] used to describe the indentation process in an elastic-plastic solid consists of hemispherical heavily deformed hydrostatic core with radius equal to indentation size. This core acts as a non-deforming "punch" into plastically deforming bulk material, again forming a hemisphere. The whole is supported by the elastically deformed hinterland. The analysis gave the following equation.

$$H^{-n/3} - H_0^{-n/3} = A_2\left(t^{1/3} - t_0^{1/3}\right)\exp\left(-\frac{Q}{3k_BT}\right) \qquad (2.15)$$

where, H is the hardness at time t, H_0 is the initial hardness at time t_0, which is taken to be on the order of 1 second, and A_2 is a constant.

Atkins [22] assumed a value of 10 for the stress exponent n and analyzed the indentation creep data on this basis. If the term t_0 and H_0 is neglected then eq. 3.3 reduces to

$$H^{-n/3} = A_1 t^{1/3} \exp\left(\frac{Q}{k_BT}\right) \qquad (2.16)$$

Roebuck and Almond [28] suggested that the direct comparison of the compression and indentation creep data is possible if the hardness values are modified to remove the effect of constrain factor from the measured hardness values since measured hardness value is approximately three

times the uniaxial yield stress of material. They suggested that this factor be included when analyzing indentation creep data as well.

Sargent and Asbhy [29] adopted a dimensional analysis approach. The stress and stress field in the material below the indenter were assumed to follow a steady-state power law. Their analysis gave the following relation between indentation hardness under creep condition and the time of loading.

$$\frac{H(t)}{\mu} = \frac{(\sigma_0 / \mu)}{\left(n\, c \dot{\varepsilon} t\right)^{1/n}} \tag{2.17}$$

Here H(t) is the time dependent hardness, μ is shear modulus, σ_0 - reference stress at which the strain rate is $\dot{\varepsilon}_0$ with indentation time t and constant c.

Li et al [30] presented a numerical simulation of the indentation creep response considering the combined effect of various deformation processes and concluded that the response is dominated by dislocation glide due to high stress involved in indentation loading.

Prakash [31, 32] extended the approach of Sargent & Ashby to include the effect of microstructural inhomogeneities on the indentation creep response of materials. Formation of dislocation sub-structures and the interaction of dislocation with second phase etc. gives rise to internal stresses which must be overcome for creep to take place. These effect have been incorporated in conjunction with the power law creep equation. Close correspondence between indentation creep and uniaxial creep response of a number of materials was demonstrated.

2.4.2 Current Work

Although the various approaches to analyze indentation creep data are successful to varying degree they all make use of the empirical power-law creep equation. None of them include explicitly the effect of thermal activation on materials subjected to high compressive stresses. A material under indentation loading is subjected to high compressive stresses (including hydrostatic component of stress) and steep stress gradient. A consideration of the pressure dependence of flow stress and thermally activated deformation is important. An approach, which incorporates some of these issues, is presented in the following chapter.

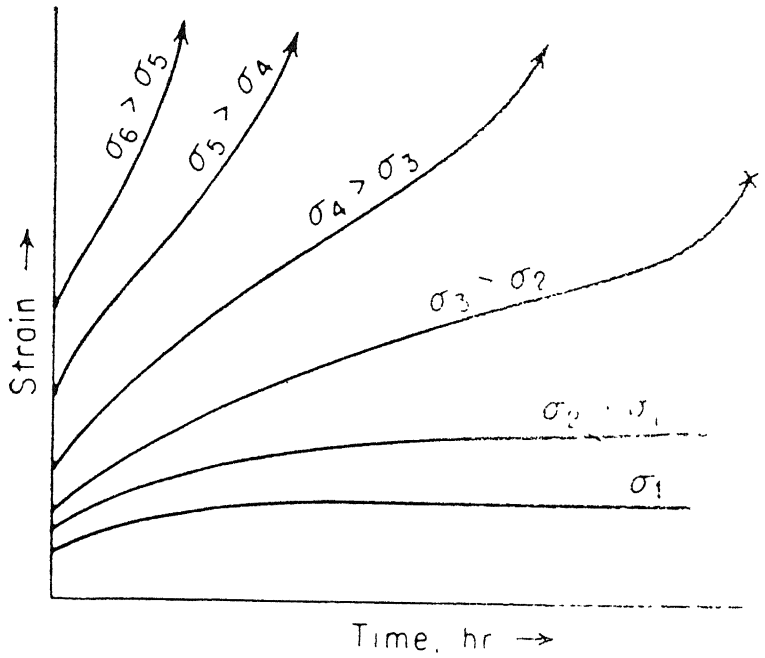

Fig.2.1: Schematic representation of creep curve at constant temperature but at different load

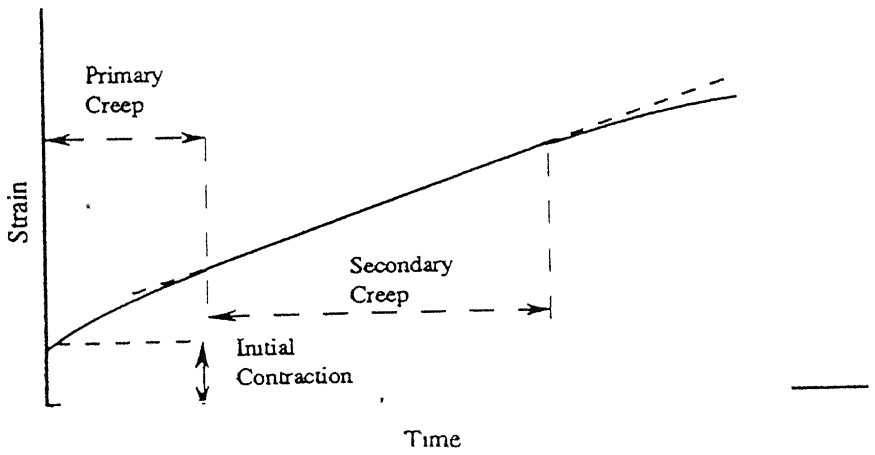

Fig 2.2: Typical creep curve for crystalline material tested in compression

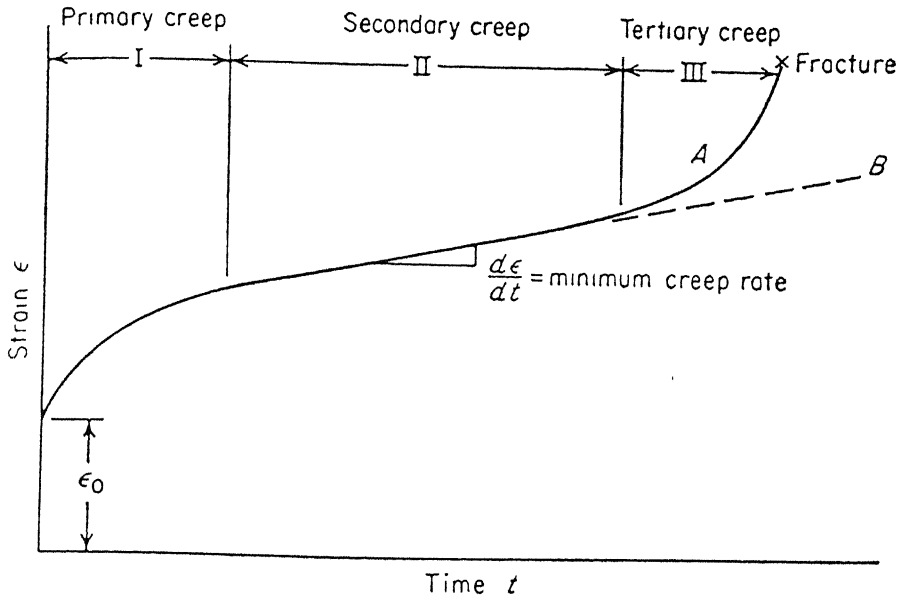

Fig 2.3: Typical creep curve for crystalline material in tension.
curve A-constant load test, curve B-constant stress test

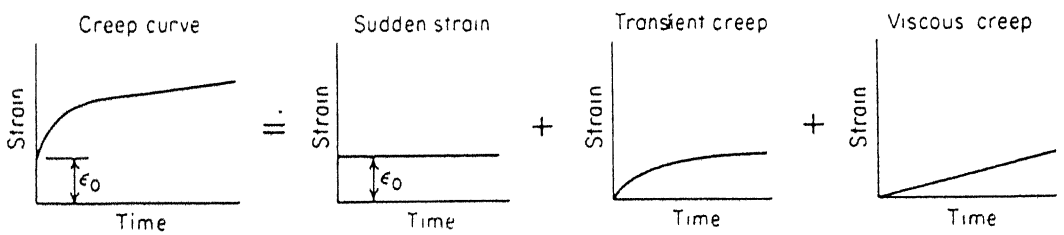

Fig2.4: Andrade's analysis of competing processes which determine the creep curve

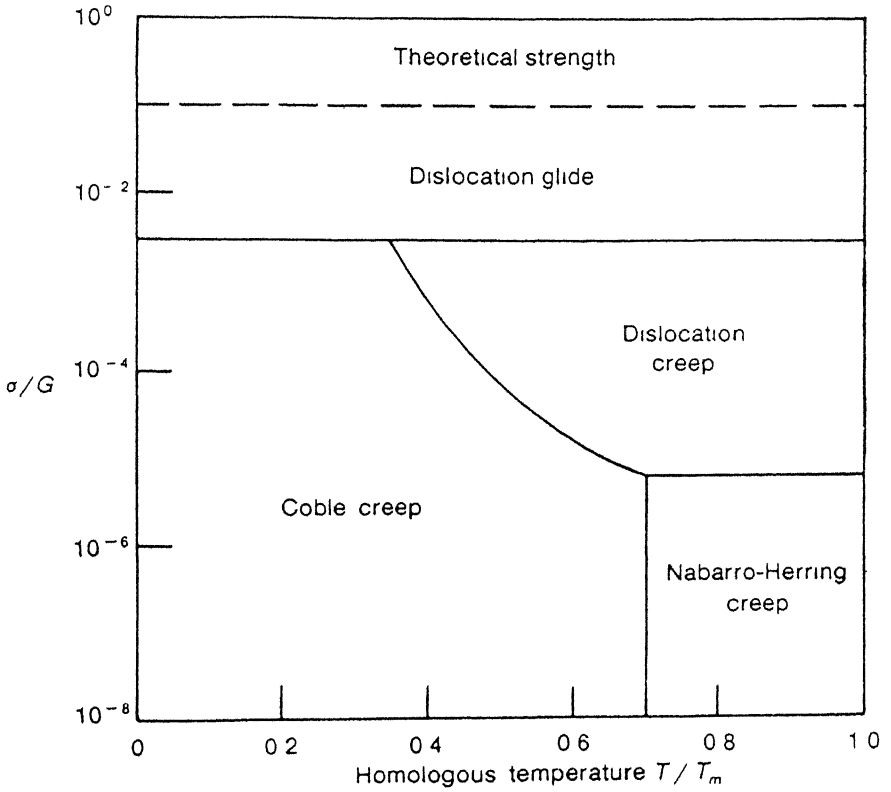

Fig 2.5: Simplified deformation mechanism map (After Ashby)

CHAPTER 3

ACTIVATION VOLUME APPROACH IN INDENTATION CREEP

3.1 Activation Volume

Activation volume is an important quantity, which can give valuable information on deformation mechanism because it has a definite value and stress dependence for each atomistic process. The variation of activation volume with temperature gives information about the deformation mechanism. Before we present a model which incorporates activation volume in indentation creep, we discuss about stress and strain field in indentation.

3.2 Stress Field Beneath the Indenter

A continuous description of the stress field beneath the Vicker's indenter and the manner in which the plastic zone evolved are of interest here. The case of Vickers indentation of solid, which undergoes creep deformation, is a complex situation and has yet not been solved. In the literature the problem of plastic indentation has been studied using three

different approach. They are the slip line field method, the expanding cavity model and the finite element method.

The slip line field method provides an upper bound solution to plastic deformation problems. The scope of it is limited to rigid plastic material. The analysis of indentation for this method has been carried out for various geometry [33-36]. Such solutions are able to explain the empirical relationship $H = 3\sigma_y$ between the indentation hardness H and uniaxial yield stress σ_y of material. However, the simplified picture of slip line field often falls short of describing the actual plastic zones involved, even for assumed rigid plastic material property.

The expanding cavity model is semi-empirical approach. It has been applied mainly to elastic-plastic materials. Tabor [37] developed a correlation between mean contact pressure associated with indentation and the yield stress. Later Johnson [38] extended this approach to include the effect of indenter geometry. His formulation provides the most comprehensive description of the correlation between experimental result of hardness and this approach. The spherical cavity expansion model has its limitation that it cannot be applied for indenter with small included angle. The third approach is that of finite element method. In contrast to the simplifying assumption regarding indenter geometry and material property required in above two approaches, this method enable one to obtain detailed solution of indentation problem for realistic stress strain relation and indenter shapes. The problem of conical indentation of elastic plastic material was analyzed by Bhatacharya and Nix [39]. Their results indicated that the shape of plastic zone depends on the ratio of elastic modulus to yield stress (E/σ_y) and the indenter angle. These shapes always differ from those assumed in the slip line theory and sometimes differ from predicted hemisphere shapes of expanding cavity model. For

material with high value of E/σ_y, the deformation mode is one of radial compression, whereas for material with low value of E/σ_y, deformation occurs by cylindrical compression. For intermediate values a combination of cylindrical and radial compression is found to take place. The shape of plastic zone is found not to change with depth of indentation.

Based on the above results that the mode of deformation for blunt indenter is that of radial compression (except for low value of E/σ_y) and is independent of the depth of material undergoing indentation creep. The stress distribution in material has a radial symmetry about indenter and that this symmetry is maintained as the material creeps. In other words, the shape of plastic zone in indentation creep is assumed to be described by and expanding hemisphere.

Since different stress level exist in the material at different distance from indenter, different creep mechanism may be dominant at different distance. This would result in strain incompatibilities with time unless continuous stress redistribution takes place. We do not know the manner in which this takes place. However, this is not a serious problem from the point of view of interpreting the creep behaviour of materials.

3.3 Indentation Creep Measurement

The indentation creep measurement consist of making separate indentation size measurement at constant load as a function of dwell time on material surface. The rate of change of hardness with time can be calculated from these measurements. The measurement corresponding to boundary $r(t) = a(t)$ in Fig. 3.1 (another boundary may be visualized at

r(t) = c(t) beyond which the stress state is elastic). In other words, the stress and strain rate of material contained in volume element r(t) = a(t) is recorded in indentation test. The control volume (CV) moves into material with increasing time (r(t)=a(t) increases with time). Now since the evolution of stress and strain rate is known in CV at all times, the creep characteristics n and Q of material may be obtained by applying the creep law to this CV only. This implies that as long as we are interested in obtaining only creep characteristics of material from indentation creep test, we do not need to know the manner in which strain compatibility is achieved. Knowledge of strain compatibility necessary only if complete description of the stress and strain field beneath indenter is required. For indentation by Vicker's indenter, hardness is given by

$$H = g\frac{P}{D^2} \tag{3.1}$$

where g is constant depending on geometry, P is applied load and D is length of indentation diagonal. Following the Roebuck and Almond [28], the applied stress, σ, at the boundary r(t) = a(t) is taken as

$$\sigma = \frac{H}{3} \tag{3.2}$$

and the strain rate at boundary r(t) = a(t) is given by

$$\dot{\varepsilon} \propto \frac{1}{D}\frac{dD}{dt} \tag{3.3}$$

using eq. 2.6 it can be shown that $\frac{1}{D}\frac{dD}{dt}$ is proportional to $-\frac{1}{H}\frac{dH}{dt}$

Therefore, the strain-rate can also be expressed as

$$\dot{\varepsilon} = -K_1\frac{1}{H}\frac{dH}{dt} \tag{3.4}$$

where, K_1 is proportionality constant.

3.4 Activation Volume in indentation creep

The stresses involved in indentation creep are usually much higher than those employed in uniaxial creep test. Under such conditions the contribution of thermal activation to plastic deformation can be small compared to the contribution of stress activation. The deformation is weakly affected by temperature when flow process is dominant. The stress and temperature dependence of strain rate is given by well known power law equation 2.3.

But it was observed by various workers that log (strain-rate) versus log(stress) plots deviates from straight line in contrast to the expected variation based on Arrhenius law and may not be suitable for creep behaviour. Gasdaska [40] and more recently Hazim and White [41] proposed a new model where the creep rate increases with the hyperbolic sine of the stress which is based on Eyring absolute reaction theory. According to it, strain rate is given by

$$\dot{\varepsilon} = AT \sinh\left(\frac{V_a \sigma}{k_B T}\right) \exp\left(-\frac{Q}{k_B T}\right) \tag{3.5}$$

where V_a is apparent activation volume, $V_a\sigma$ is work done by applied stress. For moderate stress and narrow temperature range, the negative exponential term in the hyperbolic sine and T outside the hyperbolic sine contribute negligibly and equation 3.5 simplified to exponential form

$$\dot{\varepsilon}_s = A \exp\left(-\frac{Q + V_a \sigma}{k_B T}\right) \tag{3.6}$$

or

$$\ln\left(\frac{\dot{\varepsilon}_s}{A}\right)+\frac{Q}{k_BT}=\frac{V_a\sigma}{k_BT} \tag{3.7}$$

The physical basis for these expression has already been described in section 2.3. As discussed in equation 3.4 that strain rate is proportional to $-\frac{1}{H}\frac{dH}{dt}$, and

$$\dot{\varepsilon}_s=-K_1\frac{1}{H}\frac{dH}{dt} \tag{3.8}$$

Stress σ is related to hardness by relation

$$\sigma=\frac{H}{3} \tag{3.9}$$

therefore equation 3.7 may be written as

$$\ln\left[\frac{1}{A}\left(-K_1\frac{1}{H}\frac{dH}{dt}\right)\right]+\frac{Q}{k_BT}=\frac{V_aH}{3k_BT}$$

or

$$\ln\left(-\frac{1}{H}\frac{dH}{dt}\right)+\ln K_1-\ln A+\frac{Q}{k_BT}=\frac{V_aH}{3k_BT}$$

or

$$\ln\left(-\frac{1}{H}\frac{dH}{dt}\right)+B=\frac{V_aH}{3k_BT} \tag{3.10}$$

where B is a constant. The plots of $\ln\left(-\frac{1}{H}\frac{dH}{dt}\right)$ versus $\frac{H}{k_BT}$ represent a straight line with slope $\frac{V_a}{3}$ and intercept B. Although the intercept for different materials at different temperatures may vary because it depends upon many factors but it will not affect the activation volume of material at that particular temperature. This approach may therefore be used to determine activation volume from indentation creep data.

A modified form of equation (3.6) which includes the hydrostatic pressure dependence of $\dot{\varepsilon}$ is often used by Poirier[58]

$$\dot{\varepsilon}_S = A\exp\left(\frac{-Q + V_a\sigma + VP}{k_B T}\right) \qquad 3.11$$

where V is the activation volume (based on hydrostatic pressure dependence) and P is hydrostatic pressure. In indentation, hydrostatic pressure is proportional to indentation pressure, therefore resulting equation for analysis of creep data will be similar to equation (3.10) where V_a should then be replaced by $(V_a + \alpha V)$ where α is a proportionality constant relating P to σ. However, P is not an independent variable in indentation creep. Variation in P with time takes place during indentation creep as a consequence of expansion of deformation zone which itself is controlled by thermally activated processes. The rate of change of P must therefore be consistent with the rate of expansion of deformation zone in term of geometrical compatibility requirements. One can therefore use either the term $V_a\sigma$ or VP in the above equation but when analyzing indentation creep but not both.

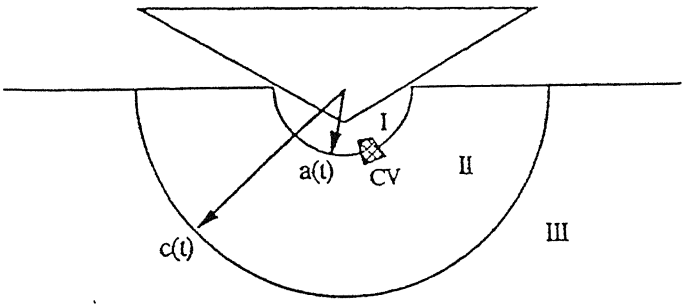

Fig.3.1 Stress distribution in indentation creep. The stress field in the material is assumed to have a radial symmetry about the indenter, and the shape of plastic zone(II) is assumed to be hemispherical. The creep measurement corresponds to change in control volume CV at r(t)=a(t).

CHAPTER 4

RESULT AND DICUSSION

In this chapter we use the approach proposed in chapter three to analyze indentation creep data of the following materials; AgCl, LiF, Fe, Si, Ge, UO_2 etc. The data has earlier been reported in literature by various authors and had been analyzed using different approaches.

4.1 Literature Data

The indentation creep data of different materials (silver chloride, lithium fluoride, iron, silicon, germanium and uranium dioxide) at different temperature are given in Table 4.2-4.7. All data pertains to measurements performed using Vickers Pyramid indenter.

Table 4.1: Shear Modulus of various materials at different temperature (based on Frost and Ashby [42])

S.No.	Material	Temperature (K)	Shear Modulus (μ in MPa)
1	LiF	293	4.58×10^4

Contd....

Table 4.1 continued....

S.No.	Material	Temperature (K)	Shear Modulus (μ in MPa)
2	LiF	373	3.89×10^4
3	UO_2	373	9.31×10^4
4	Fe	644	5.23×10^4
5	Fe	755	4.86×10^4
6	Fe	866	4.48×10^4
7	Si	1173	6.11×10^4
8	Si	1273	6.08×10^4
9	Ge	873	4.84×10^4
10	Ge	1073	4.71×10^4
11	Ge	1173	4.65×10^4

Table 4.2: Variation of Vickers micro-hardness with indentation time at different temperature for AgCl (data source: Walter W. Walker [43])

S. No.	Indentation Time (sec)	Hardness (MPa)	
		Temperature 293K	Temperature 373K
1	5	6.2	5.0
2	10	6.1	4.9
3	20	6.0	4.8
4	55	5.9	4.7

Contd....

Table 4.2 continued....

S. No.	Indentation Time (sec)	Hardness (MPa)	
		Temperature 293K	Temperature 373K
5	100	5.8	4.6
6	75	5.7	-
7	315	5.5	-
8	1000	5.4	4.2
9	1620	5.2	4.0
10	3160	4.8	3.6
11	6920	4.5	3.3

Table 4.3: Variation of Vicker's micro-hardness with indentation at a different temperature for LiF (data source: Walter W. Walker [43])

S. No.	Indentation Time (sec)	Temperature 293 K		Temperature 373 K	
		H (MPa)	$H/\mu x10^{-3}$	H (MPa)	$H/\mu x10^{-3}$
1	10	104	6.8	80	5.5
2	39	102	6.7	74	5.1
3	100	100	6.5	66	4.5
4	282	90	5.9	60	4.1
5	500	85	5.6	58	4.0

Contd....

Table 4.3 continued....

S. No.	Indentation Time (sec)	Temperature 293 K		Temperature 373 K	
		H (MPa)	$H/\mu x10^{-3}$	H (MPa)	$H/\mu x10^{-3}$
6	1000	78	5.1	56	3.8
7	1430	74	4.8	-	-
8	1832	72	4.7	54	3.7
9	2300	-	-	52	3.5
10	4285	68	4.4	-	-
11	10000	66	4.3	50	3.4

Table 4.4: Variation of Vicker's hardness with indentation time at 373K for UO_2 (data source: Walter W. Walker [43])

S. No.	Indentation time (sec)	H (MPa)	$H/\mu x10^{-3}$
1	100	520	1.67
2	290	440	1.41
3	575	425	1.36
4	1000	420	1.35
5	1800	400	1.28
6	3665	385	1.24
7	6605	375	1.20

Table 4.5: Variation of Vicker's micro-hardness with indentation time at different temperature for iron (data source: Steel and Donachie [44]

S. No.	Indentation Time (sec)	Temperature 644K		Temperature 755K		Temperature 866K	
		H (MPa)	H/μ x10^{-4}	H (MPa)	H/μ x10^{-4}	H (MPa)	H/μ x10^{-4}
1	10	908	5.20	510	3.14	287	1.92
2	32	826	4.74	468	2.88	248	1.66
3	100	787	4.51	442	2.72	237	1.58
4	275	749	4.29	383	2.36	215	1.43
5	2755	650	3.72	330	2.03	170	1.13
6	20230	590	3.38	300	1.85	147	0.98
7	60000	535	3.06	274	1.69	127	0.85

Table 4.6: Variation of Vicker's micro-hardness with indentation time at different temperature for silicon (data source: Okada et al [45])

S. No.	Indentation Time (sec)	Temperature 1173 K		Temperature 1273 K	
		H (MPa)	H/μx10^{-2}	H (MPa)	H/μx10^{-2}
1	32	575	2.82	465	2.29
2	60	550	2.70	432	2.13
3	316	500	2.45	375	1.85
4	870	468	2.29	350	1.72
5	1832	445	2.18	325	1.60

Table 4.7: Variation of Vicker's micro-hardness with indentation time at different temperature for germanium (data source: Okada et al [45])

S.No.	Indentation Time (sec)	Temp.873K		Temp.1073K		Temp.1173K	
		H (MPa)	$3H/\mu$ $x10^{-2}$	H (MPa)	$3H/\mu$ $x10^{-2}$	H (MPa)	$3H/\mu$ $x10^{-2}$
1	28	658	4.07	390	2.48	256	1.65
2	57	592	3.66	350	2.23	196	1.26
3	285	533	3.30	285	1.81	137	0.82
4	810	480	2.97	256	1.63	117	0.75
5	1670	432	2.67	230	1.46	100	0.65

4.2 Analysis of Activation Volume

The activation volumes of above listed materials are determined using the approach outlined in chapter three. They are then compared to the activation volume determined by other researchers using different testing techniques. The plots of $\ln\left(-\frac{1}{H}\frac{dH}{dt}\right)$ versus $\frac{H}{k_B T}$ are shown in Figs. 4.7-4.12 at different temperatures. The points mostly follow a linear trend. Although in some cases like LiF, it is somewhat away from the best fit curve. This is because each point represents a single hardness measurement instead of an average value of three or more indentations. Generally, the microhardness can vary by 5-10% if the experiment is repeated under similar condition on account of factors such as microstructural details, crystallographic orientation of the grain being

indented, presence of grain boundaries and others heterogeneities, fluctuation in temperature, inertia of the loading system etc.

The slope of $\ln\left(-\frac{1}{H}\frac{dH}{dt}\right)$ versus $\frac{H}{k_B T}$ directly gives the activation volume.

The activation volume data of different materials at different test temperature are given in Table 4.9.

Table 4.8: Materials, their melting points, Burger vector(b), crystal structure and their bonding

S. No	Material	Melting point	BurgerVector (Å)	Structure	Bonding
1	AgCl	728	3.15	FCC (NaCl)	Ionic
2	LiF	1140	2.87	FCC (NaCl)	Ionic
3	Fe	1530	2.48	BCC	Metallic
4	Si	1687	3.83	FCC (Diamond)	Covalent
5	Ge	1211	3.99	FCC (Diamond)	Covalent
6	UO_2	3080	3.89	Flurite (CaF_2)	Covalent

Table 4.9: Activation volume of various materials at different test temperatures

S.No	Material	Temperature (K)	T/T_m	Activation Volume (b^3)
1	AgCl	293	0.40	1548.0

Contd....

Table 4.9 continued....

S.No	Material	Temperature (K)	T/T_m	Activation Volume (b^3)
2	AgCl	373	0.51	1440.0
3	LiF	293	0.26	54.0
4	LiF	373	0.33	126.0
5	Fe	644	0.42	37.8
6	Fe	755	0.49	66.6
7	Fe	866	0.56	115.2
8	Si	1173	0.70	23.4
9	Si	1273	0.75	25.2
10	Ge	893	0.72	9.0
11	Ge	1073	0.88	14.4
12	Ge	1173	0.96	18.0
13	UO_2	373	0.12	9.0

4.3 Discussion

The variation of hardness versus indentation time at different temperature for various materials are shown in Fig.4.1-4.6. The analysis of activation volume has been carried out on the basis of approach already discussed in section 3.4. These are represented in Fig 4.7-4.12. The results indicate that activation volume generally increases with increasing test temperature for the various materials being considered in this study. The increase in activation volume can be explained on the basis of Eyring model of solid flow. It can be understand from Fig.(4.18).

If stress σ is applied to the specimen then it experiences a traction σA, where A is effective area of segment over which stress is acting. When a segment jumps, it moves to a new site which is separated from initial site by activation energy barrier Q and the distance from initial site to the barrier x. So the traction does work $(\sigma A)x$,as the segment moves to the top of the barrier. This work is absorbed by moving segment so that the energy required to facilitate the jump in forward direction becomes $(Q-\sigma Ax)$ and in backward direction $(Q+\sigma Ax)$ The quantity Ax has the dimension of volume

$$V_a = Ax \tag{4.1}$$

and is known as activation volume.

At temperature T_1 a segment acquires the sufficient amount of energy to excite to point P_1 corresponding to distance x_1 similarly at higher temperature T_2 it moves to point P_2 at distance x_2. Since the distance x_2 (at higher temperature T_2) is greater than x_1 (at lower temperature T_1) therefore $(Ax_2 > Ax_1)$, if segment area A remains same at both temperatures. Hence activation volume at higher temperature is larger than that at lower temperature.

The activation volume has been expressed in terms of the unit volume b^3 for each material. It is useful to consider the test temperature in term of homologous temperature and normalized shear stress (Fig.4.14 to 4.17).

AgCl-Although other materials show that activation volume increases with increasing temperature, AgCl shows, a reverse trend where activation volume decreases with increasing temperature i.e., 1548 b^3 at 293K (T/T_m=0.40) and 1440 b^3 at 373K (T/T_m= 0.51). But it is consisted with the results of Lloyd and Tangri [46,47]. In this temperature range they also showed using uniaxial tests that activation volume decreases

with increasing temperature Fig [4.13] In high temperature region 293-373K, the decrease in activation volume is attributed to the increase in strain-rate sensitivity. The result proposed by Lloyd and Tangri shows that at very low temperature activation parameters were independent of strain, and the rate controlling mechanism in this region were suggested to be independent of structure. So the possibility of dislocation-dislocation interaction, cross-slip, jog-drag can be ruled out. The possibility of Peierls stress was also eliminated because the relevant activation volume is only exhibited below 160 K as proposed by Dorn[48]. At room temperature the deformation is associated with pencil glide.

LiF-In this case the test temperatures are 293K and 373K which correspond to homologous temperature 0.26 and 0.33. Using deformation mechanism map (Fig. [4.14], Frost & Ashby [42]) the rate controlling mechanism appears to be plasticity. Since we are considering strain accumulation with time, the appropriate mechanism, therefore, appears to be plasticity limited by lattice resistance. However, there may also be some contribution of dislocation creep because points lie close to the boundary between plasticity and power-law creep regime.

UO_2-Uranium dioxide posses' fluorite (like CaF_2) type structure. It can be thought of an fcc stacking of metal ion with oxygen ion in the tetrahedral hole. Due to large size of uranium it diffuse more slowly. At low temperature the fluorite structure oxide shows a substantial lattice resistance, which dominates the mechanical strength upto 0.4 T_m. This in addition to low homologous temperature may be the reason behind very low activation volume of UO_2. Since for UO_2 micro hardness data at different temperatures are not available, hence variation of activation volume with temperature could not be shown.

. **Si and Ge-** The temperature dependence of Ge microhardeness involve at least two different mechanisms. At low temperature the mechanism is relatively time and temperature independent whereas at high temperature mechanism is highly time and temperature dependent. As the indenter contacts the semiconductor surface, it rapidly sinks into the material until the shear stress (or pressure) in the vicinity of the indenter falls below a critical stress (or pressure) required for deformation to proceed by means of the low temperature process. At this stage however zero time indentation (hardness impression) may now be enlarged by plastic flow resulting from strongly time and temperature dependent process.

There are two possible mechanisms, which may account for zero time indentation in Ge. It has been suggested by Gillman [49] Gridneva et al [50] that the large hydrostatic pressure under indenter may causes the crystal to undergo the pressure sensitive semiconductor to metal phase change which has been reported by Bundy [51], Phillips [52], Bust and Royce [53], Morita and Soma [54] .The metallic phase is assumed to be much less resistant to plastic flow and therefore deform to produce a permanent indentation, presumably by flow of material out from under the indenter. It is possible however that, the shear stress in the region of indenter exceeds that required for athermal motion of dislocation over Peierls barrier. These mechanism would produce an indentation in the form of an extremely thin region of highly deformed material around the surface of the indentation with more deformation outside this region , and would proceed only when the magnitude of critical stress was exceeded.

After the formation of zero time indentation, the indentation enlarges by a strongly temperature and time dependent dislocation glide process. This is a direct consequence of plastic flow by thermally

activated motion of the dislocations in Ge. Similar description is valid for Silicon.

The silicon and germanium structure can be thought of an fcc structure with two atoms associated with each fcc atomic position. Each atom has four nearest neighbors to which it is linked by four purely covalent bonds. The low co-ordination makes it a very open structure with a low density. But inspite of this, they are enormously strong due to pure covalent bonding. The iron, silicon, and germanium data are measured at same stress. The activation volume of iron is found to be 37.8 – 115.2 b^3. This well agrees with earlier observed value 50-100 b^3 Jacky[56]. The activation volume of silicon and germanium even at extremely high homologous temperature are lower than iron. The reason behind it is highly directional covalent bond of silicon and germanium in comparison to weak metallic bond of iron. The mechanical behavior of silicon and germanium is determined by their localized, strongly directional covalent bond. It creates an exceptionally large lattice resistance for slip on all slip systems. This localized nature of bonding has other consequences, like the energy of formation and motion of point defect is large, so that diffusion (at given homologous temperature) is slower than other class of solid. A general comment about the results presented in this chapter may be made here. We have calculated activation volume based on indentation creep data and comparison with literature data (wherever available) is quite satisfactory. Linking this information to possible deformation mechanisms require the variation of V_a with temperatures (since it tells us about the process being thermal or athermal) in conjunction with consideration of its actual magnitude. This has not been completed here for want of sufficient experimental data.

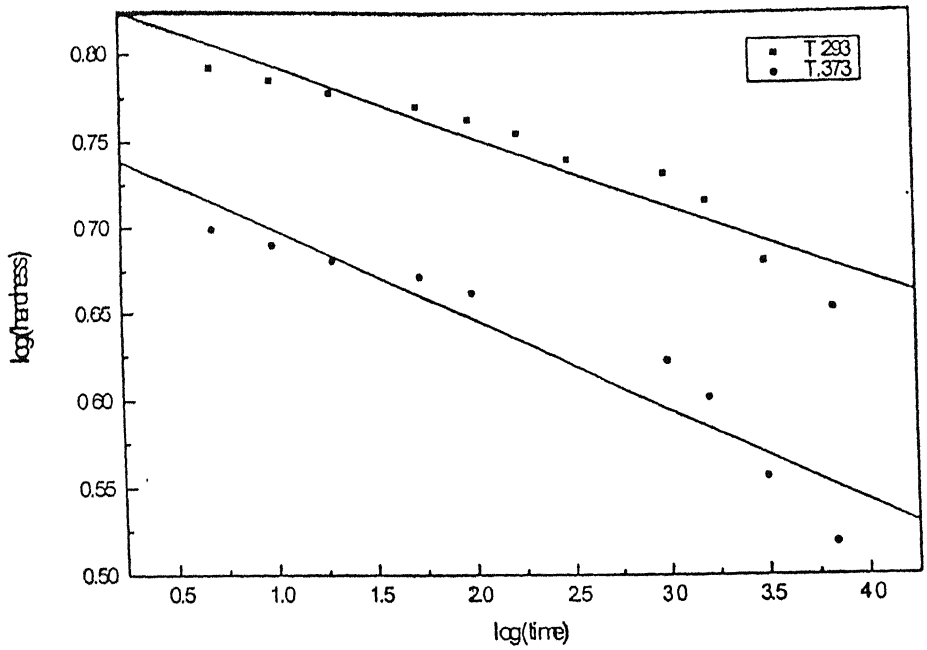

Fig. 4.1 Variation of log(hardness) Vs log(time) of AgCl at different temperature

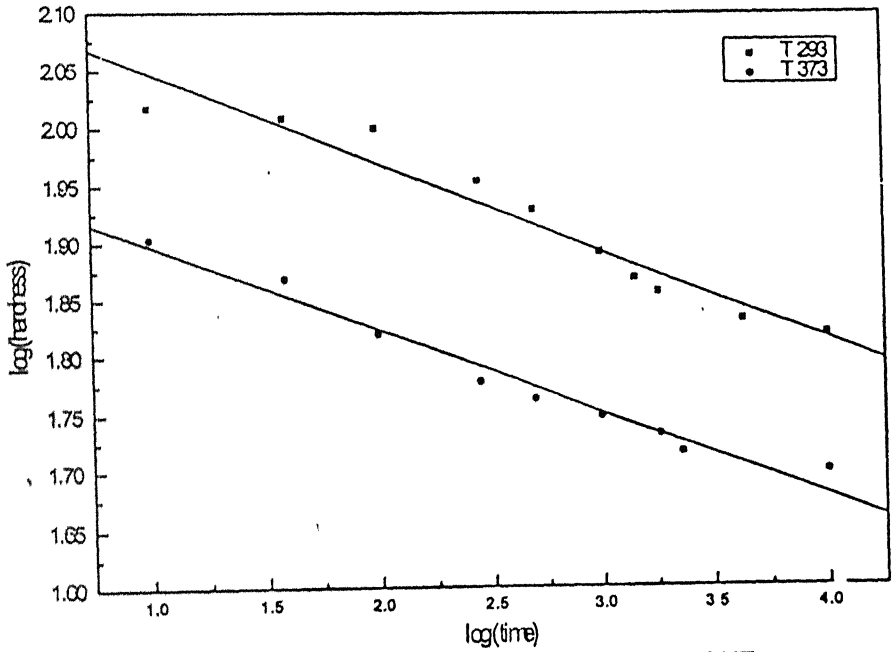

Fig. 4.2 Variation of log(hardness) Vs log(time) of LiF at different temperature

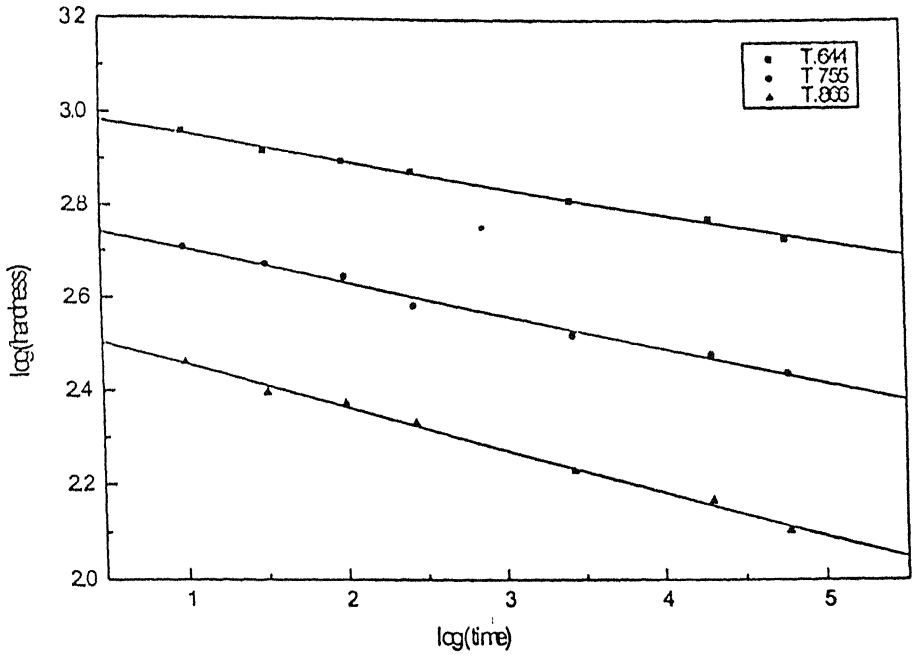

Fig. 4.3 variation of log(time) Vs log(hardness) of iron at different temperature

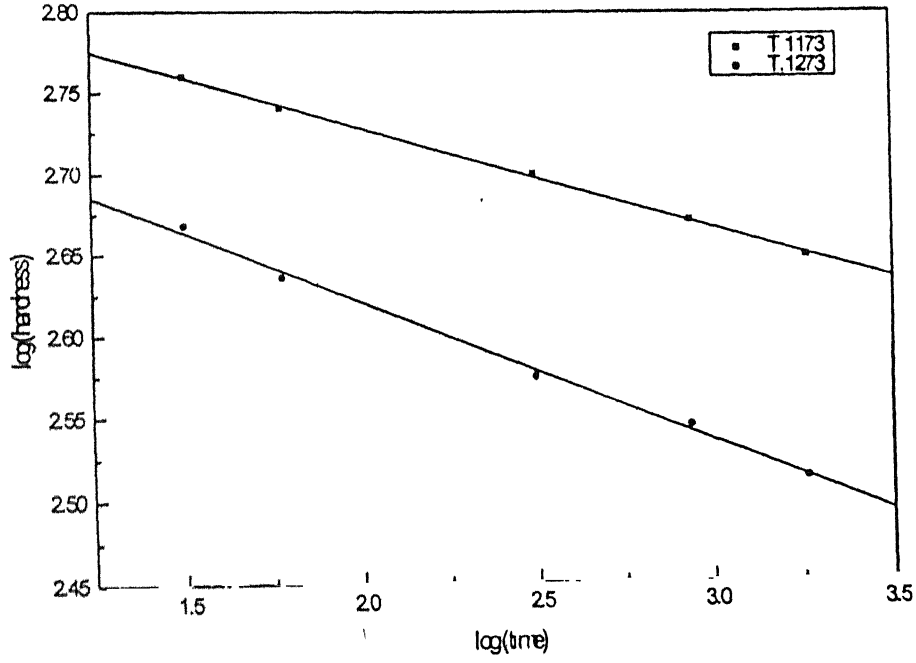

Fig. 4.4 Variation of log(time) Vs log(hardness) of silicon at different temperature

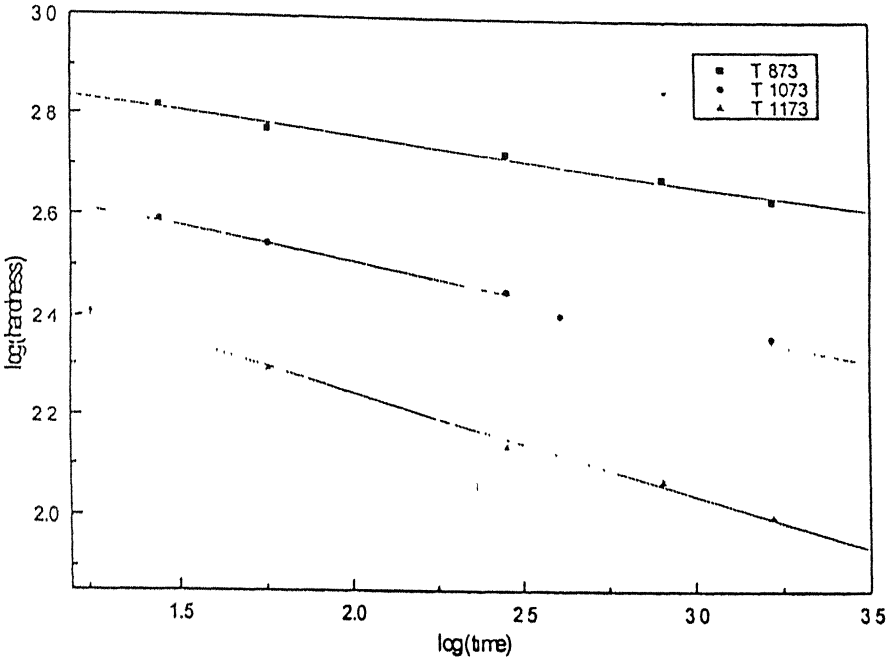

Fig. 4.5 Variation of log(hardness) Vs log(time) of germanium at different temperatures

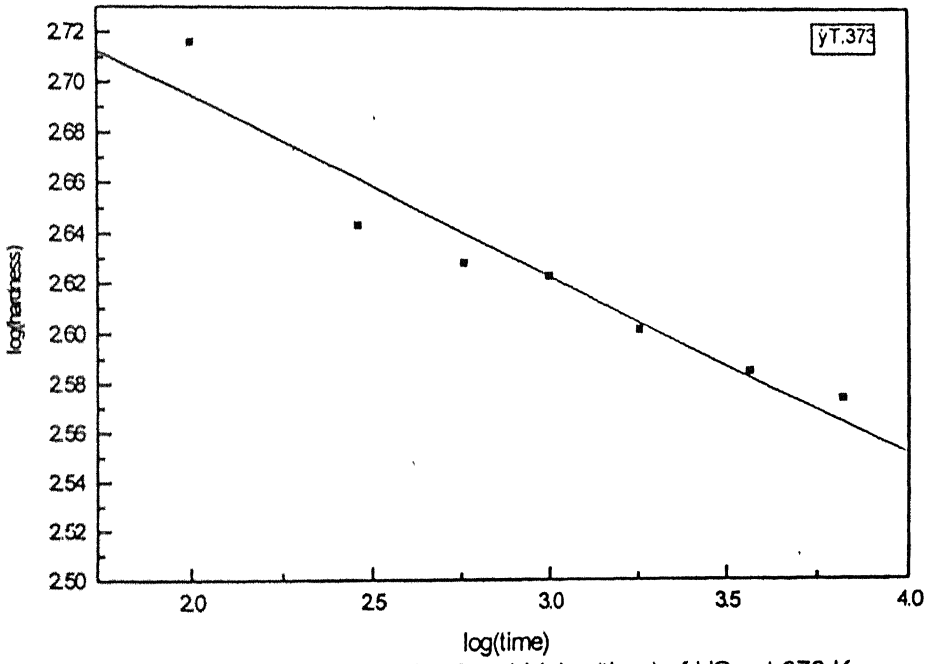

Fig. 4.6 Variation of log(hardness) Vs log(time) of UO_2 at 373 K

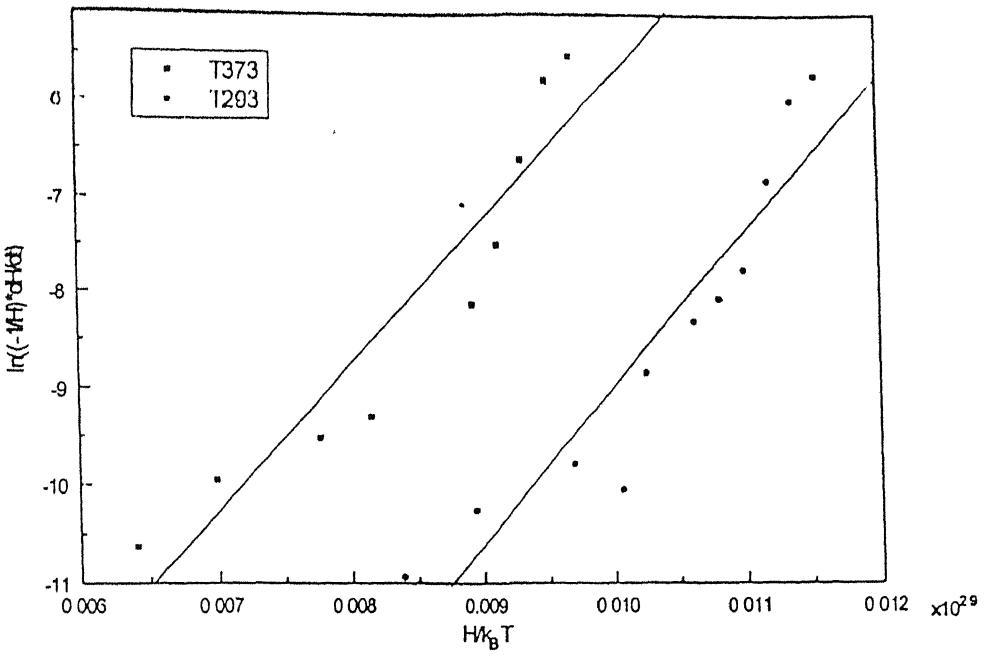

Fig. 4.7 The determination of activation volume from indentation creep data of AgCl at different temperature

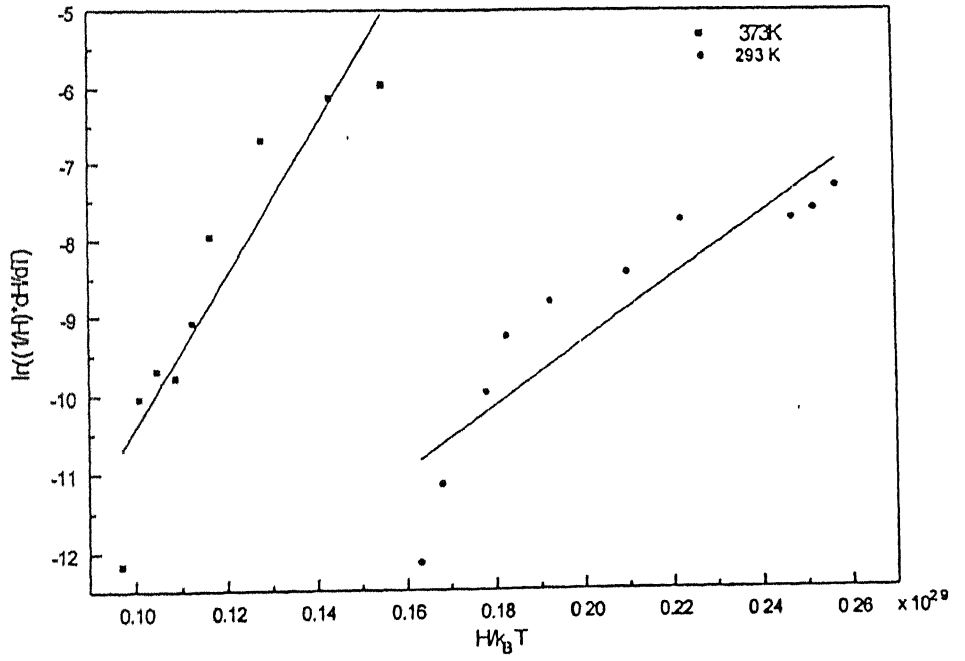

Fig.4.8 The deterimination of activation volume of LiF from indentention creep data at various temperature

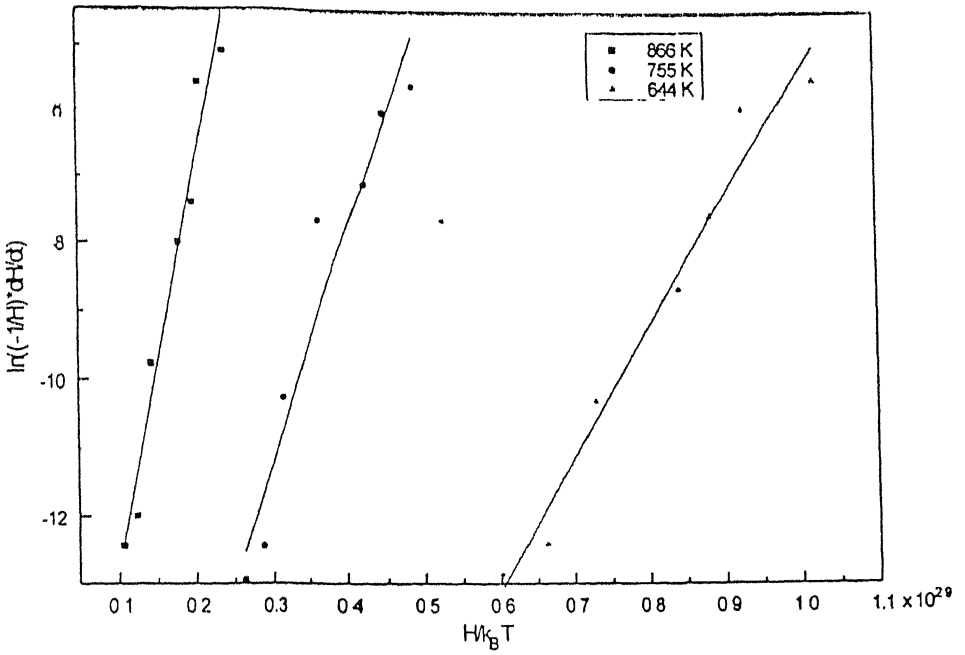

Fig 4.9 The determination of activation volume from indentation creep data of iron at different temperature

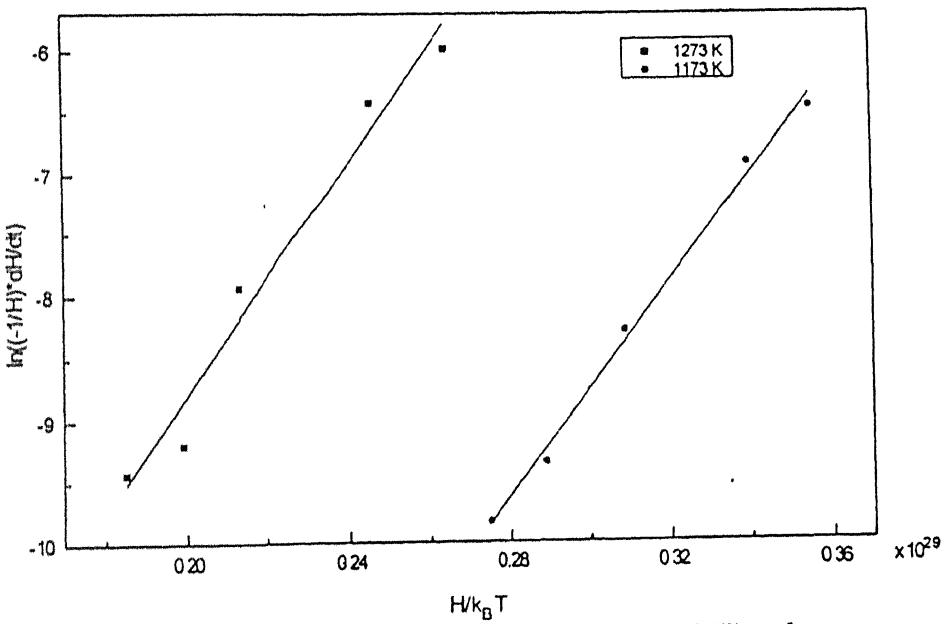

Fig.4.10 The determination of activation volume of Silicon from indentation creep data at different temperatures

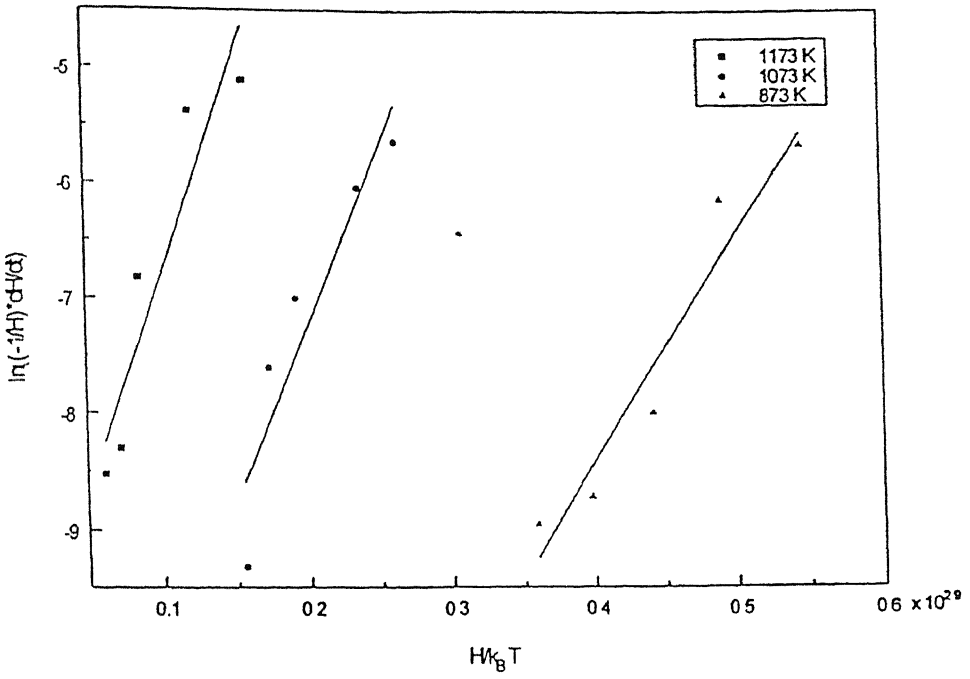

Fig 4.11 The determination of activation volume from indentation creep data of germanium at different temperature

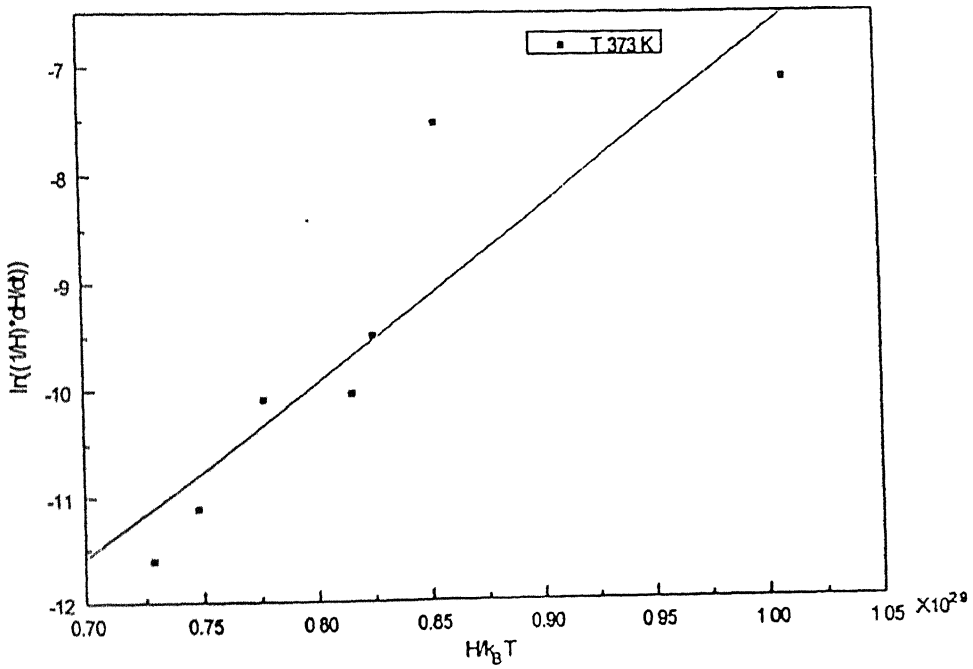

Fig. 4.12 The determination of activation volume from indentation creep data of UO_2 at 373 K

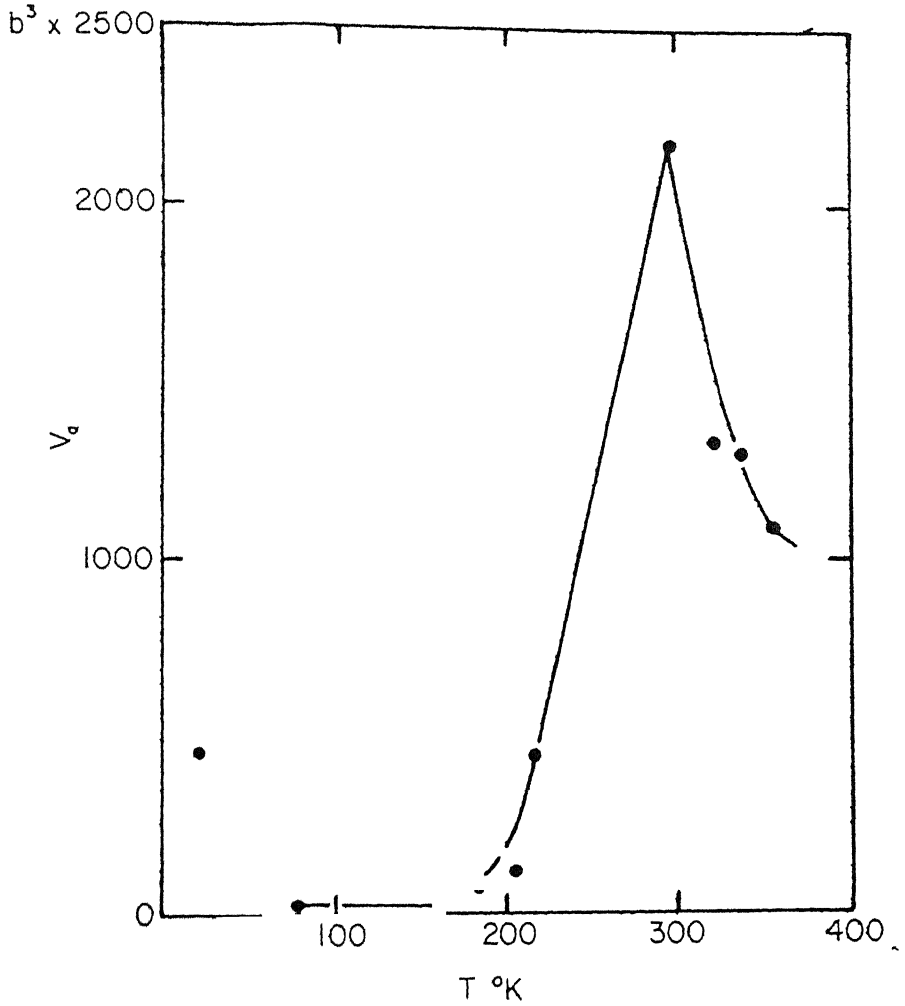

Fig.4.13: Temperature dependence of activation volume (V_a) for AgCl (Lloyd and Tangari [47]

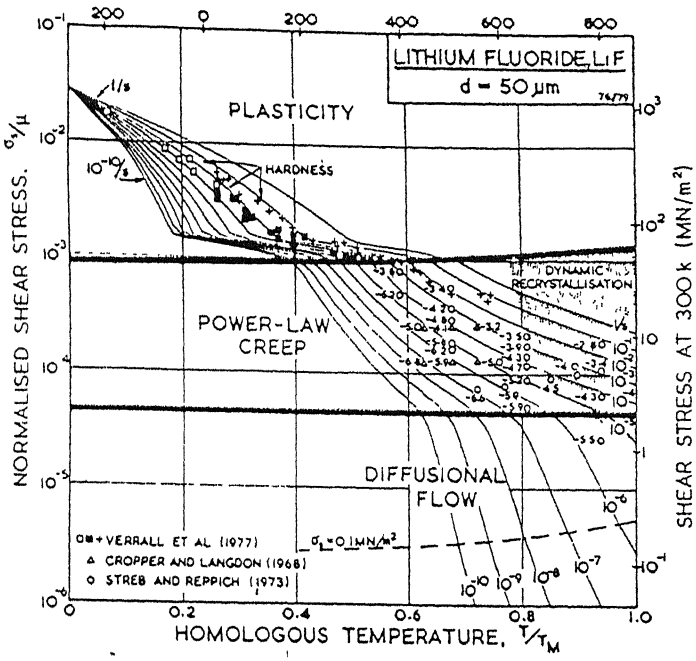

Fig. 4.14 Deformation Mechanism Map of LiF (from [42]).

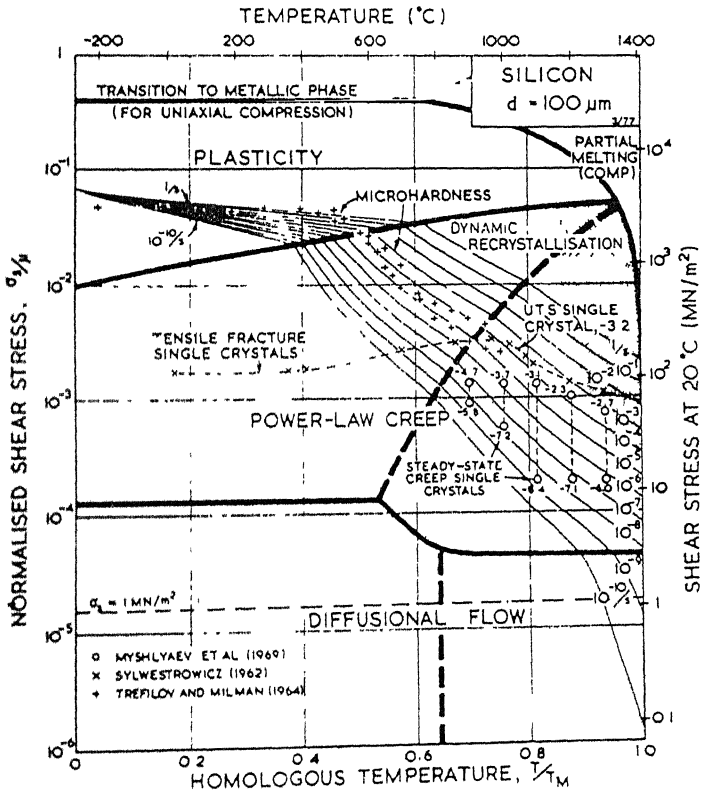

Fig. 4.15 Deformation Mechanism Map of Si (from [42]).

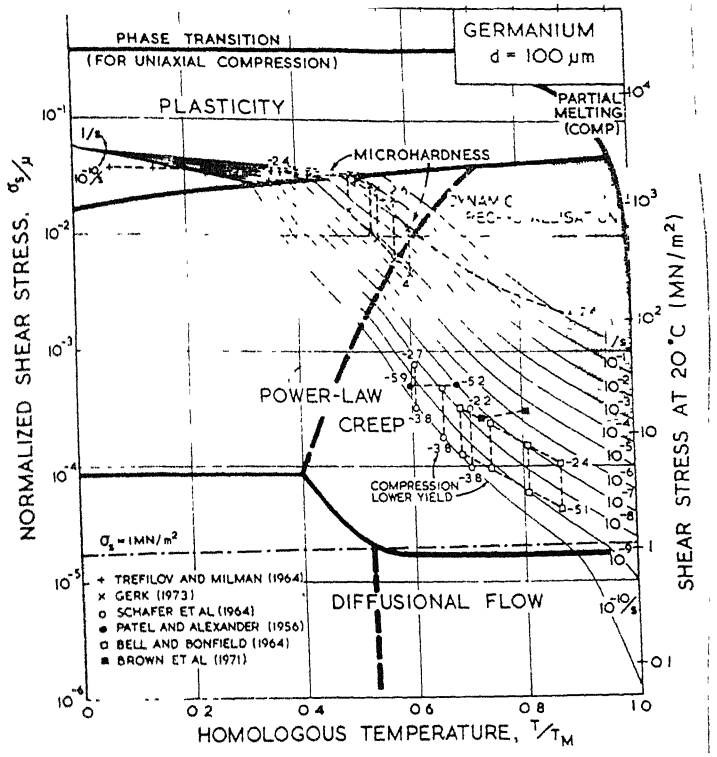

Fig. 4.16 Deformation Mechanism Map of Ge (from [42]).

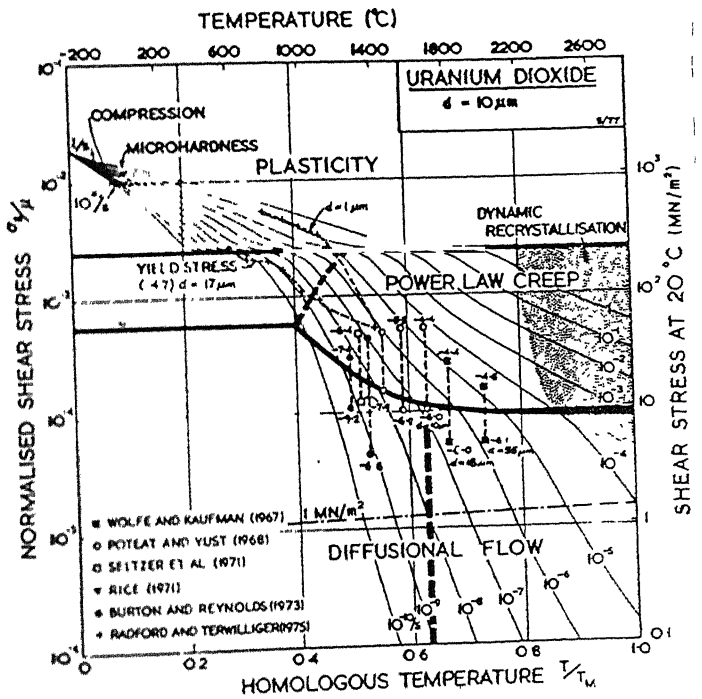

Fig. 4.17 Deformation Mechanism Map of UO_2 (from [42]).

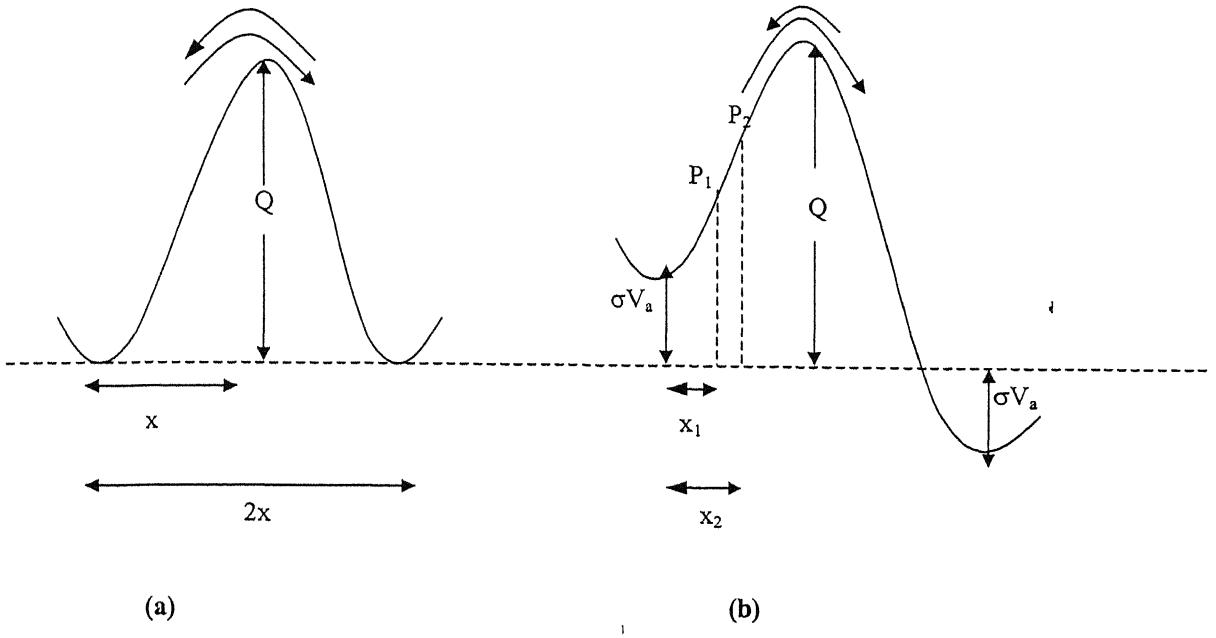

Fig 4.18- Eyring model of solid flow (a) before stress is applied to the segmant reside in potential well separated from equivalent well by (i) an activation energy barrier Q and (ii)distance 2x (b) an application of stress ,the potential well changed so that forward barrier is $(Q-\sigma V_a)$and backward barrier$(Q+\sigma V_a)$.In absence of any stress the segment jump with equal rate in forward and backward direction.

CHAPTER 5

CONCLUSION AND FUTURE WORK

5.1 Conclusion

This work has dealt with modeling of indentation creep as a thermally activated process. A procedure to extract activation volume from indentation creep data has been developed. The model has been applied to various materials for which experimental data is available in literature. The materials considered in this study are AgCl, LiF, UO_2, Si, Ge and Fe. It is found that generally the activation volume increases with increasing temperature and decreasing stress.

The activation volume of LiF, iron, silicon and germanium increases with increasing temperature. This is possibly due to increase in activation energy at same temperature range.

The small activation volume of uranium oxide is due to large size of uranium and flurite type structures and the very low homologous temperature at which lattice friction appears to be the controlling mechanism in the present study.

The creep activation volume of iron determined in the present study (37.8-115.2 b^3) is comparable to activation volume due to diffusion (50-100 b^3) as determined by earlier workers using uniaxial creep tests. A good agreement between the activation volume of two processes supports

the validity of the proposed model. The temperature range of the data for Fe is 0.42, 0.49 and 0.56 Tm.

The indentation creep response of Ge and Si is related to various factors including (i) the semiconductor to metal phase transformation as a result of the high hydrostatic pressure under the indenter, (ii) athermal motion of dislocation over the Peierls barrier as a result of the high shear stress near the indenter and (iii) the highly directional covalent bond.

5.2 Future Work

It would be useful to obtained indentation creep microhardness data for various materials in extended homologous temperature and stress ranges. This would give a clear picture of activation and better insight into the possible deformation mechanisms.

Since the idea of rate theory is quite general, the proposed approach may be used to analyze indentation creep of not just metals but also ceramics, glasses and polymers.

References:

1. E.N. da. C. Andrade and B. Chalmers, Proc. R. Soc. London; 138 A, 348 (1932)
2. R.L. Fullmann, R.P. Carreker and J.C. Fisher; Trans. AIME, 197, 657 (1953)
3. E.N. da. C. Andrade, Proc. R. Soc., London, 203, 352 (1914)
4. F. Garofalo, ASTM Spec. Tech. 282, 82 (1960)
5. E. Orowan, Proc. Phys. Soc., 52, 8 (1940)
6. S.K. Mitra and M. McLean, Proc. Royal Soc; A 295, 288 (1966)
7. R. Lagnebrg; J. Mat. Sc. 3, 596 (1968)
8. M. McLean, Proc. Roy. Soc. A 371, 279 (1980)
9. O.D. Sherby and J. Weertman, Acta Met., 27, 389 (1979)
10. S.L. Robinson and O.D. Sherby, Acta Meta., 17, 109 (1969)
11. J.P. Poirer, Rev. Phys. Appli., 11, 731 (1976)
12. J.P. Poirer, Acta Met, 26, 629 (1978)
13. J.R. Spingarn and W.D. Nix, Acta. Met., 27, 171 (1979)
14. O. Ajaja, J. Mat. Sc., 21, 3351 (1986)
15. O. Ajaja, J. Mat. Sc., 26, 6599 (1991)
16. B.Derby and M.F. Asbhy, Acta. Met., 35, 1349 (1987)
17. Ghoniem et al., Res. Mechanica, 29, 197 (1990)
18. D.S. Stone, Acta. Met., 39, 599 (1991)
19. F.Hargreaves, J. Inst. Met., 39, 301 (1928)
20. K. Ito, Sc. Rep. Tohoku Imp. Univ., 112, 137 (1923)
21. T.O. Mulhearn and D. Tabor, J. Int. Met., 89, 7 (1961)
22. A.G. Atkins, A. Silverio and D. Tabor, J. Inst. Metals, 94, 369 (1966)

23. D. Tabor, "*Microindentation Technique in Material Science*", ASTM, 889 (1986)
24. R.F. Bishop et al. Proc. Phys. Soc., 57, 147 (1945)
25. D.M. Marsh, Proc. Phy. Soc., London, A 279, 420 (1964)
26. K.L. Johnson, J. Mech. Phys. Sol., 18, 115 (1970)
27. S.S. Chiang et al, J. Appl. Phys., 53, 298 (1982)
28. B. Roebuck and E.A. Almond, J. Mat. Sc. Lett., 519 (1982)
29. P.M. Sargent and M.F. Asbhy, Mat. Sc. Tech., 8, 594 (1992)
30. W.B. Li et al, Acta Met., 39, 3099 (1991)
31. O. Prakash and D.R.H. Jones, Acta Met., 44, 891 (1996)
32. O. Prakash and D.R.H. Jones, Acta Met., 40, 3443 (1992)
33. R. Hill et al., Trans. ASME, J. Appl. Mech., 18, 46 (1951)
34. R.T. Shield, Proc. Roy. Soc., 233, 267 (1955)
35. F.J. Lockett, J. Mech. Phy. Solids, 11, 345 (1963)
36. R. Hill et al, Proc. Roy. Soc., A 188, 273 (1947)
37. D. Tabor, "*The Hardness of Metal*", Oxford university press (1951)
38. K.L. Johnson, J. Mech. Phys. Sol., 18, 115 (1970)
39. A.K. Bhatacharya and W.D. Nix, Int. J. Solids Structure, 27, 1047 (1991)
40. C.J.Gosdoska, J. Am. Soc. 78 [8], 2085, (1995)
41. R.M. Hazime and C.S.White, Ceram. Eng. Sci. Proc. 18[3], 445, (1997)
42. H.J. Frost and M.F .Ashby "*Deformation Mechanism Maps*" Pergamon Press Oxford (1982)
43. W.W. Walker, "*The Science of Hardness Testing and its Research Application*," ASM, 258, (1973)
44. R.K. Steel and M.J. Donachie, Trans. ASM, 58, 273 (1965)
45. A. Okada et al, J. Iron and Steel Inst. Japan, 73, 1186 (1987)

46. J. Gittus, "*Creep, Visco Elasticity and Creep Fracture in Solids*", Applied Science Publishers Ltd., London pp 154 (1975)
47. D.J. Lloyd and K. Tengari, Phil. Mag.,Japan, 73, 1186, (1972)
48. J.E.Dorn and S.Rajnak S.Trans.Met. Soc. AIME, 230,1052, (1964)
49. J.J. Gilman, The Science of Hardness Testing and its Research Applications, p. 51,(1973)
50. I.V. Gridman, Y.V.Millman, and V.I. Trefilov, Phys. Stat.Sol.,36,59,(1972)
51. F.P. Bundy, J.Chem. Phys., 41,3809, (1964)
52. J.C.Phillips, Phys. Rev. Lett, 27,1197, (1971)
53. W.H.Gust and E.B.Royce,J.Appl Phys, 43, 4437, (1972)
54. A.Morita and T.Soma, Solid State Commun., 11,927, (1972)
55. A.P Gerk, The Philosophical Magazin, 32, 335, (1975)
56. V. F. Zackay, "*High Strength Material*", John Willey and sons, pp 481 (1961)
57. P.A. Varotsos and K.D. Alexopoulos, "*Thermodynamics of point defects and their relation with bulk properties*", North Holland Physics Publishing (1986)
58. J.P. Poirier, "*Creep of Crystal*", Cambridge University ,Press (1985)
59. G.E. Dieter, "*Mechanical Metallurgy*", McGraw Hill Book Company (1988)
60. F.R.N. Nabarro, "*Theory of Crystal Dislocations*", Dover Publications Inc., NewYork (1987)

A-132008

Date Slip

This book is to be returned on the date last stamped.